Channel Measurements and Models for High-Speed Train Communication Systems: A Survey

Cheng-Xiang Wang, *Senior Member, IEEE*, Ammar Ghazal, *Student Member, IEEE*, Bo Ai, *Senior Member, IEEE*, Yu Liu, and Pingzhi Fan, *Fellow, IEEE*

Abstract—The recent development of high-speed trains (HSTs) as an emerging high mobility transportation system, and the growing demands of broadband services for HST users, introduce new challenges to wireless communication systems for HSTs. Accurate and efficient channel models considering both large-scale and non-stationary small-scale fading characteristics are crucial for the design, performance evaluation, and parameter optimization of HST wireless communication systems. However, the characteristics of the underlying HST channels have not yet been sufficiently investigated. This paper first provides a comprehensive review of the measurement campaigns conducted in different HST scenarios and then addresses the recent advances in HST channel models. Finally, key challenges of HST channel measurements and models are discussed and several research directions in this area are outlined.

Index Terms—High-speed train channels, channel measurements, non-stationary channel models, statistical properties.

I. INTRODUCTION

HIGH-MOBILITY scenarios, e.g., high-speed train (HST) and vehicle-to-vehicle (V2V) scenarios, are expected to be typical scenarios for the fifth generation (5G) wireless communication systems [1]. Unlike V2V communication channels that have been thoroughly investigated in the literature [2]–[10], a comprehensive study of HST communication channels is still missing. With the rapid development of HSTs, an increasing volume of wireless communication data is required to be transferred to train passengers. HST users demand high network capacity and reliable communication services regardless

C.-X. Wang and A. Ghazal are with the Institute of Sensors, Signals, and System, School of Engineering and Physical Sciences, Heriot-Watt University, Edinburgh EH14 4AS, U.K. (e-mail: cheng-xiang.wang@hw.ac.uk; ag289@hw.ac.uk).

B. Ai is with the State Key Laboratory of Rail Traffic Control and Safety, Beijing Jiaotong University, Beijing 100044, China (e-mail: boai@bjtu.edu.cn).

Y. Liu is with the R&D Center on B4G Wireless Communication Networks, School of Information Science and Engineering, Shandong University, Shandong 250100, China (e-mail: xinwenliuyu@163.com).

P. Fan is with the Institute of Mobile Communications, Southwest Jiaotong University, Chengdu, Sichuan 610031, China (e-mail: p.fan@ieee.org).

of their locations or speeds. To satisfy these demands, HST wireless communication systems have to overcome many challenges resulting from the high speed of the train that can easily exceed 250 km/h, such as fast handover, fast travel through diverse scenarios, and large Doppler spreads [11], [12] besides some challenges inherited from conventional trains such as high penetration losses, limited visibility in tunnels, and the harsh electromagnetic environment [13].

Since 1998, the Global System for Mobile Communication Railway (GSM-R) has widely been adopted as Europe standard for train communications and control. However, GSM-R can only provide a data rate of up to 200 kbps [14], besides the fact that it is mainly used for train control rather than providing communications for train passengers [15]. Therefore, GSM-R cannot meet the requirements for future high speed data transmissions [16] and International Union of Railways has recommended that GSM-R has to be replaced by long-term evolution-Railway (LTE-R) [17]–[23], which is a broadband railway wireless communication system based on LTE-Advanced (LTE-A) [24]. Nevertheless, both systems still adopt the conventional cellular architecture where mobile stations (MSs) inside trains communicate directly with outdoor base stations (BSs). Such an architecture leads to a spotty coverage and high penetration losses of wireless signals traveling through the metal carriages of HSTs. In addition, the receiving signals at MSs on board will experience fast changing channels resulting in high signaling overhead and high possibility of drop calls and handover failure [25].

The aforementioned problems can be mitigated by deploying other cellular architectures, such as distributed antenna system (DAS) [26]–[28], coordinated multipoint (CoMP) [29], [30], mobile relay station (MRS) [31]–[34] (or mobile femtocell [1], [35], [36]) technologies, or a combination of these architectures, e.g., DAS with MRS [37] or CoMP with MRS [38]. In a DAS, distributed antenna elements are connected to a BS via wires or fibers (radio over fibers (RoF)) [39], [40] to provide considerable gain in coverage and capacity in comparison with the conventional cellular architecture. The spatially separated antenna elements can be used to transmit the same signal at different locations to provide spatial diversity against the fading. Combined with spatial diversity, frequency reuse in the DAS is an effective technique to increase system capacity. The enhancement in spectral efficiency of DASs in comparison with conventional systems was presented in [26]. In [27], the authors analyzed the deployment of DAS over HST communication systems and some of the resulting problems such as the coverage of the remote antenna units (RAUs) and echo channel
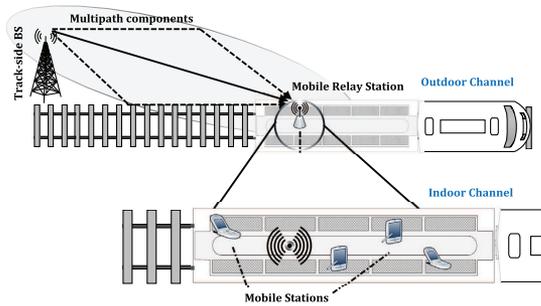
Fig. 1. A HST communication system deploying MRSs.

effect. In CoMP systems, the transmission of neighboring BSs will be coordinated in the downlink while the received signals at the uplink will be jointly processed. This will reduce the inter-cell interference and improve the cell edge throughput. CoMP systems will also provide an enhanced channel capacity by using the statistically independent properties of the channels resulting from the wide spatial separation of antenna elements. Adopting mobile femtocell architecture in HST communication systems can be performed by deploying dedicated MRSs on the surface of the train to extend the coverage of the outdoor BS into train carriages. As a result, we will have two channels: an outdoor channel between the BS and MRS, and an indoor one between the MRS and an MS of a train passenger as illustrated in Fig. 1. In this case, the BS will mainly communicate with the MRS at high data rates instead of communicating with large numbers of MSs directly. An MRS and its associated MSs within a train carriage are all viewed as a single unit to the BS, while the MSs will see the relevant MRS as a regular BS. It follows that an MRS can perform a group handover on behalf of all its associated MSs, which can greatly reduce the frequent handover burden of the HST system [36]. Since the complexity of radio resource allocation (i.e., transmit power, data rates, scheduling, power and frequency allocation, and antenna selection) in a BS is related to the number of active users [26], the radio resource management complexity in one BS will be reduced significantly when dealing with a "group of users" rather than individuals. This promising MRS technology has been adopted by IMT-Advanced (IMT-A) [41] and WINNER II [42] channel models.

Moreover, the transmitter (Tx) and receiver (Rx) of a HST wireless communication system encounter different channel conditions due to the difference of surrounding geographical environments. The HST environment can be generally classified into the following main scenarios: open space, viaduct, cutting, hilly terrain, tunnels, and stations. Considering some unique setup of the aforementioned scenarios and some other special HST scenarios, HST environment can be further classified into 12 scenarios [43]. HSTs can operate across one or more of these scenarios during its travel. The propagation characteristics change significantly with the change of environments and the distance between the Tx and Rx, even in the same terrain. Scenarios have a close relationship with channel modeling and measurements. Most standard channel models in the literature, like UMTS [44], COST 2100 [45], and IMT-2000 [46], failed to introduce any of the HST scenarios. The moving

networks scenario in the WINNER II channel model [42] and rural macro-cell (RMa) scenario in the IMT-A channel model [41] have only considered a rural environment for HSTs, while neglecting other HST scenarios. The aforementioned propagation scenarios will be introduced and explained in detail in Section II.

The features of HST channels, e.g., non-stationarity and large Doppler shift, significantly differ from those of low-mobility mobile cellular communication channels. Therefore, many measurement campaigns have been conducted in the literature to understand the underlying physical phenomenon in HST propagation environments. Accurate channel models that are able to mimic key characteristics of wireless channels play an important role in designing and testing HST communication systems. Realistic and reliable large-scale fading channel models, i.e., path loss (PL) and shadow fading (SF) models, are indispensable for efficient and trustworthy network deployment and optimization. Small-scale fading channel models are crucial in physical layer design in order to develop and test different transmission schemes, such as diversity of transmission/reception, error correction coding, interleaving, and equalization algorithms. Inaccurate channel models may lead to over-optimistic or over-pessimistic performance evaluation results that will result in misjudgments in product development. Moreover, inaccurate channel models may lead to inaccurate link budgets that will result in huge errors of the estimated maximum distance between adjacent BSs. Consequently, this will cause poor coverage and increased drop calls due to failed handovers between BSs when the distance is underestimated, and unnecessary overlapped coverage area with unjustified installation and maintenance cost of the extra installed BSs when the distance is overestimated [47]. In the literature, several large-scale and small-scale fading HST channel models were proposed. This article will focus on the recent advances in HST channel measurements and modeling and their future challenges.

The rest of this paper is organized as follows. In Section II, an overview of HST channel measurements is provided. The state-of-the-art of HST channel models is presented in Section III. Future research directions in HST channel measurements and models are outlined in Section IV. Finally, concluding remarks are highlighted in Section V.

II. HST CHANNEL MEASUREMENTS

Special attention has been given to HST channel measurements in recent years. Due to the high speed of the train and the hostile HST environments, conducting accurate channel measurements for HST communication systems is challenging and needs to address particular hardware and software requirements, e.g., robustness, scalability, hardware redundancy and traceability [48]. Many measurement campaigns [49]–[93] for different HST environments were presented in the literature. Here, we will briefly review and classify the important measurements for HST communications according to the scenarios, cellular architecture, measurements' setup parameters (i.e., antenna configuration, carrier frequency, and bandwidth), and measured channel statistics, as shown in Table I.

TABLE I
IMPORTANT HST CHANNEL MEASUREMENTS

Ref.	Cellular Architecture	Scenario	Carrier Frequency	Bandwidth	Antenna	Train Speed	Channel Statistics
[49]	MRS	N/A	2.2 GHz / 5.2 GHz	20 MHz	SISO	270 km/h	PL
[50]	MRS	N/A	2.35 GHz	100 MHz	SISO	N/A	PL, DS, K
[51]	Conventional	Open space	2.6 GHz	20 MHz	SISO	370 km/h	PL, DS, DF, PDP
[52]	Conventional	Open space	2.5 GHz	50 MHz	MISO/SIMO	290 km/h	DS, AoA, AoD, PAS, DF
[53]	Conventional	Open space	5.2 GHz	120 MHz	SIMO	350 km/h	PL, SF, K, DS, PDP, AS
[54]	MRS	Open space	930 MHz	200 kHz	SISO	350 km/h	PL, SF
[55]	MRS	Viaduct	930 MHz	200 kHz	SISO	340 km/h	PL, K
[56]	MRS	Viaduct	930 MHz	200 kHz	SISO	N/A	PL
[57], [58]	MRS	Viaduct	930 MHz	200 kHz	SISO	300 km/h	K
[59]	MRS	Viaduct	930 MHz	200 kHz	SISO	350 km/h	PL, SF
[60]–[62]	MRS	Viaduct	930 MHz	200 kHz	SISO	350 km/h	PL
[63], [64]	MRS	Viaduct	930 MHz	200 kHz	SISO	350 km/h	SF
[65]	MRS	Viaduct	930 MHz	200 kHz	SISO	300 km/h	PDF, LCR, AFD, CDF, FM
[66]	MRS	Viaduct	2.35 GHz	10 MHz	SISO	240 km/h	PL, DS, K
[67]	MRS	Viaduct	2.35 GHz	50 MHz	SISO	196 km/h	DS, K, SF
[68], [69]	MRS	Viaduct	930 MHz	200 kHz	SISO	360 km/h	PL, K, SF, FD, LCR, AFD
[70]	MRS	Viaduct	2.6 GHz	20 MHz	SISO	370 km/h	PL, SF, DS, K
[71], [72]	MRS	Viaduct	2.35 GHz	50 MHz	SISO	200 km/h	PSD, DF, AoA, K
[73]	MRS	Cutting	930 MHz	200 kHz	SISO	320 km/h	PL, SF
[74]	MRS	Cutting	930 MHz	200 kHz	SISO	350 km/h	PL, K
[75]	MRS	Cutting	930 MHz	200 kHz	SISO	295 km/h	K, FD
[76]	MRS	Cutting	930 MHz	200 kHz	SISO	350 km/h	PL, K, SF, FD, LCR, AFD
[77]	MRS	Cutting	2.35 GHz	50 MHz	SISO	200 km/h	PL, K, SF, DF
[78]	MRS	Cutting	2.35 GHz	50 MHz	SISO	200 km/h	DS, DF
[79], [80]	Conventional	Hilly Terrain	2.4 GHz	40 MHz	SISO	295 km/h	PL, SF, K
[81]	Conventional	Tunnel	2.154 GHz	30 MHz	SISO	N/A	PL, DS
[82]	MRS& DAS	Tunnel	930 MHz	200 kHz	SISO	N/A	PL
[83]	MRS	Station	930 MHz	200 kHz	SISO	N/A	PL
[84]	MRS	Station	930 MHz	200 kHz	SISO	N/A	PL, K, SF, FD, LCR, AFD
[87]	MRS	Various	930 MHz	200 kHz	SISO	350 km/h	PL, PDF, DS, PDP
[88]	MRS	Various	930 MHz	200 kHz	SISO	340 km/h	SI
[89], [90]	MRS	Various	930 MHz	200 kHz	SISO	340 km/h	SF
[85]	MRS	Various	930 MHz	200 kHz	SISO	290 km/h	K, LCR, AFD
[91], [92]	MRS	Various	2.1 GHz	3.84 MHz	SISO	240 km/h	PL, K, DS, PDP
[93]	Conventional	Various	2.1 GHz	3.84 MHz	SISO	300 km/h	PL, PDP

SISO: single-input single-output; MISO: multiple-input single-output; SIMO: single-input multiple-output; PL: path loss; DS: RMS delay spread; K: Ricean K-factor; PDP: power delay profile; AS: angular spread; AoA: angles of arrival; AoD: angles of departure; PAS: power azimuth spectrum; DF: Doppler frequency; SF: shadow fading; FD: fade depth; LCR: level crossing rate; AFD: average fade duration; PDF: probability density function; CDF: cumulative distribution function; FM: fading margin; PSD: power spectrum density; SI: stationarity interval

A. HST Propagation Scenarios

HST environments can be roughly classified into the following 6 scenarios: open space, viaduct, cutting, hilly terrain, tunnels, and stations.

1) In the open space scenario [52], also called plain scenario [51], the Rx is moving at a very high speed in a rural area where the BS antenna is much higher than the surroundings [54]. This environment focuses on large cells and continuous coverage where the link between the fixed Tx and moving Rx normally has a dominant line-of-sight (LoS) component. However, after a certain distance, called breakpoint distance, the impact of the sparse scatterers will be noticed at the Rx represented by non-LoS (NLoS) components. As a result, the slopes of the PL and Ricean K-factor will be noticeably changed at the breakpoint leading to dual-slope PL model [94]. It has been proved that there is a strong link between the breakpoint distance and the antenna height. For a certain site, as the antenna height decreases, the breakpoint moves closer to the Tx. This is because a bigger Fresnel zone is intercepted by the ground, usually covered by vegetation, when the antenna height is lower. Furthermore, due to the influences of different environments, slight variations in the breakpoint distance can be noticed in different scenarios. Therefore, it can be concluded that the breakpoint distance is mainly determined by the antenna height
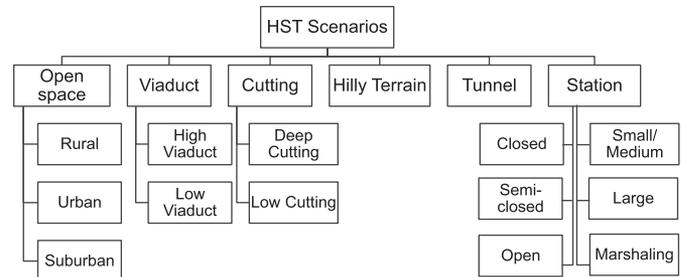

Fig. 2. Classification of HST scenarios.

while slightly affected by environments [95]. Based on the geographic nature and the distribution/height of the surrounding scatterers, the open scenarios can be further classified into rural [53], urban, and suburban scenarios as illustrated in Fig. 2.

2) The viaduct scenario is very common for HSTs [55]–[71]. The main purpose of viaducts is to ensure the smoothness of the rail and the high speed of the train. In this scenario, the radio reflection, scattering, and diffraction caused by nearby scatterers, e.g., trees and buildings, can also be reduced significantly. The viaduct height and relative BS height have great influence on the received signal. Because of the relatively high altitude

TABLE II
HST SCENARIOS

Scenario	Description	LoS/NLoS	Key Parameters
Open Space	Can be further classified into rural, urban, and suburban scenarios	LoS	Density/height of surrounding scatterers
Viaduct	A bridge that ensures the smoothness of the rail. High speeds of the train can be achieved. Radio reflection, scattering, and diffraction can be reduced. Can be classified into high and low viaducts	LoS	Height of the viaduct; BS' height relative to the viaduct's height; Height of surrounding scatetterers
Cutting	A U-shaped geographical cut that ensures the smoothness of the rail; The propagation of radio waveforms is significantly affected by the steep walls and the vegetation on both sides of the cutting. Can be classified into deep and low cuttings	LoS	Dimension of the cutting; Height of the cutting; MRS' height relative to the cutting's height
Hilly terrain	The surrounding environment is densely scattered with objects distributed irregularly and non-uniformly.	LoS	Density/height of surrounding scatterers
Tunnel	Has unique propagation characteristics different from those of other HST scenarios; Waveguide phenomena is present. Suffers from limited visibility	LoS/NLoS	Length, size, and shape of the tunnel
Station	Can be classified according to the size or architecture	LoS/NLoS	Size of the station Stations' architecture

of the viaduct in comparison with the surrounding terrain, the LoS component is dominant in this scenario. However, the sparsity of the scatterers in the environment around the viaduct will still influence the received signal at the Rx [59]. Based on the relative altitude between the scatterers and the viaduct, this scenario can be further classified into high viaduct and low viaduct scenarios. In the former, most scatterers located within 50 m from the viaduct are lower than the surface of the viaduct and therefore their impact on the propagation characteristics is negligible. In the low viaduct scenario [71], [72], some of the nearby scatterers are higher than the surface of the viaduct and consequently they introduce rich reflections and scattering components that may result in a severe shadow fading and/or extra pathloss [43].

3) The cutting scenario is another common scenario for HST wireless communications [73]–[78]. It represents an environment where the HST passes a U-shaped geographical cut surface between the hills. The cutting is widely used for HST construction to ensure the smoothness of the rail and help to achieve a high speed of the train when passing through hills. The propagation of radio waveforms in this scenario is significantly affected by the steep walls on both sides. The LoS component can be observed along the route of the HST in this scenario. Here, we can recognize between two cutting scenarios: deep cutting if the receive antenna mounted on top of the train is lower than the upper eave of the cutting and low cutting if the height of the upper eave is lower than the top of the receive antenna.

4) In the hilly terrain scenario [79], [80], the surrounding environment is densely scattered with objects distributed irregularly and non-uniformly. With high-altitude transmit antennas and low-altitude obstacles, the LoS component is observable and can be detected along the entire railway. However, multipath components scattered/reflected from the surrounding obstacles will cause serious constructive or destructive effects on the received signal and therefore influence the channel's fading characteristics.

5) The tunnel scenario represents an environment where HST passes through tunnels [81], [82] with different lengths ranging from hundreds of meters to several kilometers. The

length, size, and shape of the tunnels and the encountered waveguide phenomena have significant impact on the communication channel. Because of the long limited space, bounding of tunnel, and poor smoothness of the interior wall, propagation characteristics of signals in tunnels are quite different from other scenarios. To overcome the problem of the limited visibility encountered in tunnels and to design an optimal wireless communication network, leaky feeders and DAS are often deployed. However, as HSTs may require long tunnels, the leaky feeder solution is very expensive especially at high operating frequencies and its maintenance is considerably complex [96]. As a result, DAS is more practical [97]. It can provide considerable gains in coverage and capacity, and provide spatial diversity against the fading by using the antenna elements at different locations. It also has advantages in future applications such as higher distance between repeaters and easy maintenance after being opened.

6) The stations scenario represents the railway facility where HSTs stop regularly to load/unload passengers [83], [84]. HST stations can be classified according to their size or architecture. Based on the size of the station, which reflects the estimated communication traffic, station scenario can be categorized into small to medium size stations, large stations, and marshalling stations [43]. From the architecture perspective, which affects the propagation characteristics inside the station, three HST station scenarios can be recognized, i.e., open station, semi-closed station, and closed station [84] as illustrated in Fig. 2. Table II briefly summarizes the description and key-parameters of the aforementioned scenarios.

The aforementioned scenarios are the most encountered ones in HST environments. However, recent measurement campaigns have shed some light on other special HST scenarios such as crossing bridges [86]. Besides the previous "individual" scenarios, HSTs may encounter more than one scenario (the so-called combination scenario [43]) in one cell. Two combination scenarios are reported in the literature. The first one is a combination between tunnel and viaduct where viaducts are usually used as transition between tunnels in mountain environments. The frequent transition between tunnels and viaducts will increase the severity of fading at the transition points causing

a drop in the communication quality. The second combination is between cutting scenarios, i.e., deep and low cuttings, and rural scenario. The frequent and fast transition between these scenarios can degrade the quality of the communication link and makes signal prediction quite challenging.

B. Channel Statistics

Channel statistics are essential for the analysis and design of a communication system. Most of HST measurement campaigns have concentrated on large-scale fading statistics, i.e., path loss (PL) and shadowing. The measurement campaign presented in [49] studied the PL in HST channels when the Tx and Rx were located inside the same HST carriage and when they were located in different carriages. The measured results showed that the waves traveling inside the same train carriage are dominant compared to the ones reflected from scatterers outside the HST due to the high penetration loss of wireless signals traveling through the metal body of the carriages. On the contrary, the waves reflected from outer scatterers are dominant compared to the waves traveling inside the train carriages when the communication devices are located in different carriages due to the high insulation between these carriages. In [50], the PL of indoor wideband HST channels was also investigated using two different indoor Tx configurations, i.e., omni-directional antenna mounted on the ceiling of the HST and a planner antenna mounted on the wall of the carriage. Measurements showed that the channel between the Tx planner antenna and Rx can suffer 10 dB greater loss compared with the one between the Tx omni-directional antenna and Rx. The aforementioned results from both measurement campaigns are very useful for the design of HSTs and measurement scenarios. However, more measurements for indoor scenarios in HSTs are needed before confirming that these observations are conclusive. PLs of HST channels in open space and hilly terrain scenarios were reported in [51], [53], [54] and [79], [98]. Measurement data reported in both hilly terrain scenarios showed a breakpoint in the estimated PLs. A dominant and strong LoS component can be easily observed before the breakpoint while the impact of scatterers starts and grows beyond the breakpoint distance. The breakpoint distance depends on the clearance of the first Frensal zone and can be calculated based on the Tx and Rx antenna heights and the wavelength of the transmitted signal [42]. Therefore, different breakpoint distances were reported in the aforementioned hilly terrain measurements, i.e., 778 m in [79] and 500 m in [98]. Since viaduct is a common HST scenario, the PL of HST viaduct channels has thoroughly been studied in the literature, e.g., [55], [56], [59], [66], [68], [69]. Most of these measurements highlighted the impact of the height of the viaduct and the relative height of the BS on the estimated PL. In general, there are two main observations that can be concluded from the aforementioned viaduct measurements. First, the higher the BS antenna, the smaller the PL exponent for a given viaduct height. Second, the viaduct reduces the severity of the channel fading. In other words, the higher the viaduct, the less fading severity. Both observations are physically meaningful considering that the increase of the heights of the BS and the viaduct over the surrounding obstacles

will lead to a clear LoS and reduce the impact of these scatterers on the received signal. The measurements of HST channels in cutting scenarios reported in [73], [74], [76], [77] have demonstrated the impact of the cutting structure, i.e., the depth and the widths of the top and bottom of the cutting, on the estimated PLs. A shallow cutting, or low cutting, will lead to a strong LoS condition while deep cutting will lead to a large PL exponent due to the reflections from the cuttings' slopes. A comparison between the PL of cutting and viaduct scenarios was carried out in [73]. It was suggested that the propagation conditions in the cutting scenarios can be worse than those of viaduct ones because of the reflected and scattered components caused by the slopes of the cutting. It is important to note that such a conclusion is highly dependant on the dimensions of the studied viaduct and cutting, as we have highlighted the impact of those dimensions on the estimated PL earlier. On the other hand, shadowing has generally been modeled as log-normal distributed in different HST scenarios. Various channel statistics studied in HST channel measurement campaigns are shown in Table I.

The Ricean K-factor is a very important parameter in link budget and channel modeling. Therefore, many papers presented the estimation of K-factors in different scenarios, e.g., open space [53], viaduct [55], [57], [58], [66]–[69], cutting [73]–[77], and hilly terrain [79]. The previous discussions of the dominance of the LoS component, the breakpoint distance, and the impact of the viaduct and cutting structure are also related to the K-factor. For example, [69] showed how a higher value of the viaduct height will lead to a higher value of the K-factor. In the same context, it showed that lower viaducts lead to more surrounding scatterers, which results in an increase in the severity of the fading and a considerable fluctuation of the K values. Moreover, the measurement in [69] showed while the K-factor is a linear function of distance, the slopes of K values are different before and after the breakpoint. Similar comprehensive studies on K-factors of HST channels but in cutting scenarios were reported in [76], [99]. The analysis showed that wide cuttings increase the possibility of dominant LoS components, which leads to higher K-values. Distance-dependant linear K models for different cutting dimensions before and after the breakpoint distance were proposed in [76].

In [65], [68], [69], [76], the spatial/temporal variations, e.g., fade depth (FD), level-crossing rate (LCR), and average fade duration (AFD), were investigated. FD is a measure of variation in the channel energy about its local mean due to small scale fading and it is calculated from the difference in signal levels between 1% and 50%. Measurements in viaduct scenarios have shown that FD is independent of the viaduct's height but is affected by the number and closeness of surrounding scatterers that are higher than the viaduct [65], [69]. LCR is defined as the expected rate at which the received signal crosses a specified level in a positive-going or negative-going direction, while AFD is defined as the average period of time for which the received signal is below this specified level, i.e., threshold. LCR and AFD were statistically modeled as functions of the structural parameters of the viaduct and cutting scenarios in [69], [76]. The results showed that the severity of fading in viaduct scenarios is greatly reduced compared with that in open space

TABLE III
PL AND SHADOW FADING MODELS FOR HST CHANNELS

Ref.	Scenario	PL exponent (n)	Intercept (A)	SF std (dB)	Notes
[50]	Indoor	2.16 1.8	49.8 39.9	2.8 2.3	Using planner antenna at Tx Using omni-directional antenna at Tx
[42]	RMa	2.15 4	44.2 10.5 - 18.5 $\log_{10}(\frac{h_{BS}}{h_{MS}})$	4 6	30m$< d < d_{BP}$ $d_{BP} < d < 10$km
[56]	Viaduct	3.665 4.326	71.83	N/A	Open viaduct Non-open viaduct
[60]	Viaduct	$0.000194 h_{BS} + \frac{42.84}{h_{BS}} + 0.705$	85.5	2.1– 3.1	n related to h_{BS}
[61]	Viaduct	$-0.0012308 d_0 + 3.94$ $-0.0037949 d_0 + 6.4333$ $-0.00044615 d_0 + 3.596$	$20 \log_{10}\left(\frac{4\pi d_0}{\lambda}\right)$	2.1– 3.1	$200 \leq d_0 \leq 900$ $d_0 > 900$, high viaduct: $h_v > 25$m $d_0 > 900$, low viaduct: $h_v < 25$m
[62]	Viaduct	$0.000194 h_{BS} + \frac{42.84}{h_{BS}} + 0.04798 H_{BS}$	85.5	2.1– 3.1	n related to h_{BS} and H_{BS}
[66]	Viaduct	3.03	12.4	2	
[69]	Viaduct	$-0.043 h_v + 0.236$ $-0.02 h_v + 1.65$	$0.61 h_v + 91.75$ 54.95	4.93 2.47	d $\leq d_{BP}$ d $> d_{BP}$
[73]	Cutting	4.3	71.83	3.5	
[74]	Cutting	$13.05\, e^{-0.039(w_{\text{down}}-w_{\text{up}})}$ $1.66 w_{\text{down}}^2 - 58.51 w_{\text{down}} + 517.6$	85.5	4 3	Deep cutting Low cutting
[79]	Hilly Terrain	2.4 3.88	31.31 -11.6	3.3 4.2	d $< d_{BP}$ d $\geq d_{BP}$

d_{BP}: breakpoint distance; h_{BS}: BS antenna height; h_{MS}: MS antenna height; H_{BS}: BS effective antenna height; d_0: reference distance; λ: wavelength; h_v: viaduct height; w_{down} and w_{up}: cutting dimensions

scenarios, since fewer reflected and scattered paths in viaduct scenarios are expected at the receiver which leads to smaller values of LCR. Obstacles around the viaduct can cause minor variations of the LCR values but have no significant impact on the AFD. Cutting's dimensions have also very minor impact on the AFD of the received signal, while surrounding obstacles and crossing bridges over the cutting have no influence on the LCR and AFD. Doppler behavior and angular information of HST channels in open space scenarios were analyzed in [52], while power delay profiles (PDPs) were investigated in [51], [53], [87], [91], [92]. In [96], a measurement was carried out in a tunnel scenario and the signal propagation characteristics at the breakpoint were discussed.

The stationarity interval, defined as the maximum time duration over which the channel satisfies the wide sense stationary (WSS) condition, of HST channels was investigated in [88] based on measurements. It showed that conventional channel models offered stationary intervals much larger than the actual measured ones. In [100], the non-stationarity of a HST channel in a cutting scenario was investigated using a metric called non-stationarity index. The non-stationarity index was defined as the distance between the auto-correlation of a real time-variant transfer function and the auto-correlation of this transfer function under the WSS assumption. The reported measurement data showed that the non-stationarity index increases when the Doppler frequency shift varies fast. In the future, more channel statistics, especially those related to small-scale fading parameters, are necessary to be investigated in measurements.

C. Measurement's Setup Parameters

Carrier Frequency and Bandwidth: most of the measurement campaigns in the literature were conducted at the carrier frequency of 930 MHz in GSM-R systems [54]–[58], [60]–[63], [65], [68], [69], [73]–[76], [82], [87], [88]. Correspondingly, all of the aforementioned measurements were for narrowband channels with bandwidth of 200 kHz. Wideband channel measurements with higher bandwidths, i.e., 10–100 MHz, and higher carrier frequencies, i.e., 2.1–5.2 GHz, were reported in [49]–[53], [66], [67], [77]–[79], [81], [91]–[93].

Antenna Configuration: The majority of HST measurements campaigns so far have focused on single-input single-output (SISO) systems [49]–[51], [54]–[63], [65]–[69], [73]–[79], [81], [82], [87], [88], [91], [92]. Multiple-input multiple-output (MIMO) systems, where multiple antennas are equipped at both ends, are essential for providing higher capacity to meet the requirements of future high speed data transmissions [101]. The channel measurement, particularly the MIMO channel measurement at high moving speeds, remains to be a challenging task. So far, only very few measurement campaigns were conducted using multiple antennas at either the Tx, i.e., single-input multiple-output (SIMO) systems [52], [53], or Rx, i.e., multiple-input single-output (MISO) systems [52]. Hence, HST MIMO wideband channel measurement campaigns with carrier frequency and bandwidth larger than GSM-R ones are needed for future HST communication system developments.

TABLE IV
IMPORTANT SMALL-SCALE FADING HST CHANNEL MODELS

Ref.	Channel	Channel Model	Scenario	Stationarity	Antenna	FS	Scatterer Region	Cellular Architecture
[24]	Outdoor	Non-fading	Open space	Stationary	MIMO	Narrowband	N/A	Conventional
[102]	Outdoor	GBDM	Open space	Non-stationary	MIMO	Wideband	Non-isotropic	Conventional
[103]	Outdoor	GBDM	Open space	Non-stationary	MISO	Wideband	Non-isotropic	Conventional
[104]	Outdoor	GBDM	Various	Non-stationary	SISO	Narrowband	Non-isotropic	Conventional
[105], [106]	Outdoor	GBDM	Tunnel	Non-stationary	SISO	Narrowband	Non-isotropic	Conventional
[107]	Outdoor	RS-GBSM	Open space	Stationary	MIMO	Narrowband	Non-isotropic	Conventional
[108]	Outdoor	RS-GBSM	Open space	Stationary	MIMO	Wideband	Isotropic	Conventional
[109]–[111]	Outdoor	RS-GBSM	Open space	Non-stationary	MIMO	Wideband	Non-isotropic	Mobile Relay
[112]	Outdoor	GBSM	various	Non-stationary	MIMO	Wideband	Non-isotropic	Mobile Relay
[41], [42]	Outdoor	IS-GBSM	Open space	Stationary	MIMO	Wideband	Non-isotropic	Mobile Relay
[107], [113]	Outdoor	IS-GBSM	Cutting	Stationary	MIMO	Narrowband	Isotropic	Conventional
[93]	Outdoor	IS-GBSM	Open space	Non-stationary	MIMO	Wideband	Non-isotropic	Conventional
[114], [115]	Outdoor	NGSM	Open space	Non-stationary	MIMO	Wideband	Non-isotropic	Conventional
[116]	Outdoor	NGSM	Viaduct	Non-stationary	MIMO	Wideband	Non-isotropic	Mobile Relay

III. HST CHANNEL MODELS

HST channel models in the literature can be categorized as large-scale fading models [42], [50], [51], [56], [60]–[62], [66], [69], [73], [74], [77], [79] and small-scale fading models [24], [41], [42], [102]–[116]. The state-of-the-art of HST channel models has not been investigated yet. Therefore, we will first categorize PL models in Table III. In Table IV, the important HST small-scale fading channel models are briefly reviewed and classified according to the modeling approach, scenario, stationarity, antenna configuration, frequency selectivity (FS), scatterer region, and cellular architecture.

A. Large-Scale Fading Models

PL estimation is essential for wireless link budget computation and wireless network planning. PL and shadow fading channel models for various HST scenarios have been developed based on measurement results conducted in the open literature [3]–[14]. These PL models are typically expressed as

$$PL(d) = A + 10n \log_{10}(d) \quad (1)$$

where d is the distance between the Tx and Rx in meters (m), n is the PL exponent, and A is the intercept. Note that the SF follows log-normal distributions, the standard deviation of which for each model is given in Table III.

B. Cellular Architectures and Scenarios

As mentioned earlier, adopting conventional cellular architecture in HST wireless communication systems may lead to several problems in terms of providing reliable and fast communication to HST passengers. Therefore, other cellular architectures, such as DAS, CoMP, and MRS need to be considered. In the literature, most of the proposed channel models have considered the conventional architecture where fixed BSs are installed on the track-side to provide wireless coverage to HST passengers inside carriages [24], [102], [103], [105]–[108], [114]. By considering MRS solution, we will have two channels, outdoor channel between the BS and the MRS and an indoor one between the MRS and train passengers. The properties of radio channels in the carriages resemble those of indoor

environments and hence they can be modeled using existing indoor channel models [50]. Therefore, [41], [42], [109]–[111], [116] have focused on modeling the outdoor channel because of the challenges that this channel faces due to the high velocity of the Rx.

HST scenarios have been presented in details earlier in this paper in Section II. While most of these scenarios can only be encountered in railway environments, open space scenario is similar to the rural or urban scenarios that can be found in conventional V2I or V2V communication systems. Therefore, most of the current HST channel models, developed from V2I and V2V channel models by taking into account the effect of the high velocity of the Rx on the channel parameters, have been proposed for open space scenario [24], [41], [42], [102], [103], [108]–[111], [114]. Channel models for tunnel, cutting, and viaduct scenarios were studied in [106], [107], and [116].

In summary, more HST channel models that consider other cellular architectures, such as DAS, are needed in the future. In addition, more HST scenarios should be considered in proposing future HST channel models.

C. Modeling Approaches of HST Small-Scale Fading Models

In terms of modeling approaches, the current HST channel models in the literature, presented in Table IV, can be classified as deterministic [102]–[106] and stochastic channel models. The latter can be further classified into geometry-based stochastic models (GBSMs) [41], [42], [107]–[111] and non-geometrical stochastic models (NGSMs) [114], [116], as illustrated in Fig. 3.

1) Deterministic Channel Models: Deterministic channel models are usually based on the detailed description of specific propagation environment and antenna configuration. The amplitudes, phases, and delays of the propagated waves are obtained using intensive simulations that incorporate details of propagation environments like roads, buildings, trees, houses, etc. Therefore, deterministic models are physically meaningful and potentially accurate. Geometry-based deterministic models (GBDMs) based on ray-tracing method were proposed in [103]–[106] to model HST propagation channels in different HST scenarios. In [106], a three-dimensional (3D) ray-tracing
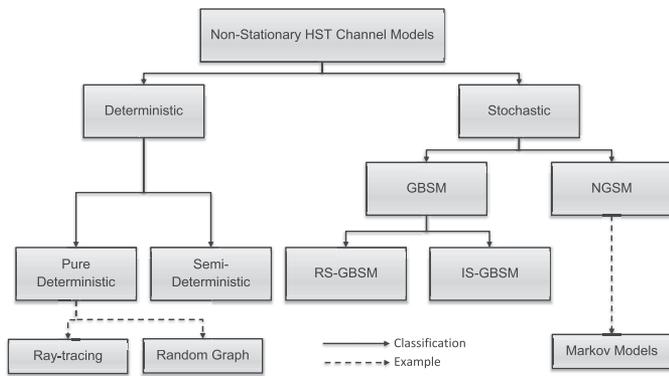
Fig. 3. Classification of non-stationary HST channel models.

Fig. 4. A RS-GBSM with LoS and single-bounced rays for a HST cutting scenario.

approach for wave propagation modeling in HST tunnels was presented. The proposed model resulted in the complex channel impulse response that incorporates channel information, e.g., the wave-guide effect observed in tunnels and the impact of another train passing in the opposite direction on the Doppler shift and time delay. The authors in [104] adopted a similar approach to model HST channels in various scenarios. Both [106] and [104] used measurement results to verify the proposed channel models. Another HST channel model based on 3D ray-tracing approach was presented in [103] to analyze channel characteristics, e.g., the FS and time-variance (Doppler spread). The objects, e.g., trees, buildings, or barriers, on both sides of the railway track were modeled using rectangular boxes, the dimensions of which were statistically generated. Since the propagation characteristics of electromagnetic (EM) waves in tunnels are significantly different from those in other HST environments, a multi-mode waveguide channel model was proposed in [117]. The proposed model, which is a hybrid model that combines the geometrical optical model and waveguide model, can characterize the wave propagation both in near and far regions of the source. However, the aforementioned model failed to discuss the far LoS (FLOS) phenomena observed inside tunnels [118] or provide a mechanism to determine the breakpoint for different propagation regions in tunnels [13]. A GBDM based on random propagation-graph was proposed in [102] to characterize time-variant HST channels in open space scenarios. Similar to ray-tracing method, propagation-graph can predict channel impulse responses by a thorough search of propagation paths that connect the Tx and Rx. This modeling approach can be performed by considering the geometry of the simulated environments, e.g., the distribution, mobility, and visibility of the scatterers. Despite their high accuracy, GBDMs require detailed descriptions of the propagation environments and extensive computational resources to be implemented. To avoid the high complexity of implementing GBDMs while maintaining sufficient accuracy, semi-deterministic models for HST viaduct and cutting scenarios were proposed in [119]. However, the proposed models only considered large-scale fading and neglected the effect of small-scale fading parameters on the received signal.

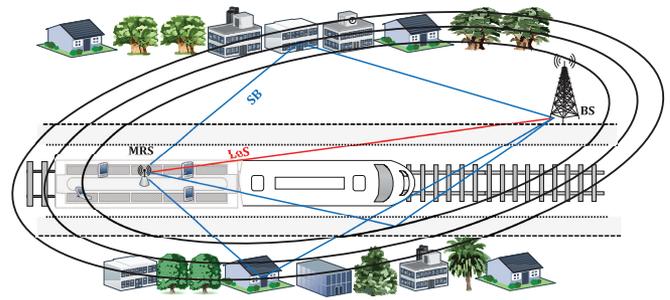*2) GBSMs:* In GBSMs, the impulse responses of HST channels are characterized by the law of wave propagation applied to specific Tx, Rx, and scatterer geometries which are predefined in a stochastic fashion according to certain probability distributions. Different types of GBSMs differ mainly in the proposed scatterer distributions. Based on the position of the effective scatterers, GBSMs can be further classified as regular-shaped GBSMs (RS-GBSM) such as one-ring [108], two-ring, and ellipse models [109]–[111], and irregular shaped GBSMs (IS-GBSMs) [41], [42], [107].

RS-GBSMs assume that all the effective scatterers are placed on regular shapes and therefore, different RS-GBSMs have different shapes of scatterer distributions, e.g., one-ring, two-ring, and ellipses for two-dimensional (2D) models and one sphere, two-sphere, and elliptic-cylinders for 3D ones. RS-GBSMs often result in closed-form solutions or at least mathematically tractable formulas. The generalized principle of designing RS-GBSMs follows the following steps. First, a geometrical model is adopted assuming that scatterers are located on regular shapes. Then, a stochastic reference model with an infinite number of scatterers is developed based on the adopted geometrical model. However, the reference model cannot be used for simulations and therefore a corresponding simulation model with a finite number of effective scatterers is needed. The parameters of the simulation model are computed by using proper parameter computation methods, e.g., the extended method of exact Doppler spread (EMEDS), modified method of equal area (MMEA) [120], or the L_p-Norm Method (LPNM) [121]. In [108], a one-ring RS-GBSM was proposed to model HST channels in open space scenarios. The scatterers were assumed to be distributed on a ring around the MS where different PDFs of the scatterers were analyzed. Considering the narrowband GSM-R for a HST communication system, a 3D one-sphere RS-GBSM was proposed in [107] for open space scenarios. The proposed model used the Von Mises distribution to describe the azimuth angles and the space-time (ST) cross-correlation function (CCF) was derived. However, both of the aforementioned models assumed that the HST channel satisfies the WSS condition that has been proved incorrect by measurements [52]. To fill this gap, non-stationary RS-GBSMs were proposed in [109]–[112] for wideband MIMO HST channels considering the deployment of MRS on the top of the train. Fig. 4 illustrates the proposed RS-GBSMs, which consist of multiple confocal ellipses with single-bounced rays and the LoS component.

The model was first introduced in [109], [110], where it considered the distance between the Tx and Rx as time-varying

to capture the non-stationarity of the HST channel. Then, the model was further developed in [111] by considering other time-varying model parameters, i.e., angles of departure (AoDs) and angles of arrival (AoAs). By adopting some key scenario-specific channel parameters, this model was further extended in [112] to be applicable to the three most common HST scenarios, i.e., open-space, viaduct, and cutting scenarios [47], and hence is the first generic HST channel model. To demonstrate its applicability, the proposed generic non-stationary HST channel model was verified by measurements in terms of stationary time for the open space scenario and the autocorrelation function (ACF), LCR, and stationary distance for the viaduct and cutting scenarios [112].

IS-GBSMs place the effective scatterers with predefined properties at random locations with certain statistical distributions usually obtained/approximated from measurements [122]. Unlike RS-GBSMs, the random locations of the scatterers do not form regular shapes and the signal contributions of the effective scatterers are determined from a greatly-simplified ray-tracing method and finally the total signal is summed up to obtain the complex impulse response. IS-GBSMs for HST channels were introduced in the RMa scenario in WINNER II [42] channel model and the moving networks scenario in IMT-A channel model [41]. In both cases, the train speed can be up to 350 km/h and the MRS technology is employed. In [107], an IS-GBSM was proposed for HST channels in cutting scenarios assuming the scatterers to be uniformly distributed on the surface of the two slopes of the cutting. However, the aforementioned channel models have neglected the non-stationarity of HST channels and assumed that the WSS assumption can still be applied. Moreover, GBSMs are very complex for upper-layer protocol design and performance analysis and less complex channel models are preferred.

3) NGSMs: NGSMs characterize physical parameters of a HST propagation channel in a completely stochastic manner by providing their underlying probability distribution functions without assuming an underlying geometry. An NGSM based on finite-state Markov chains for HST wireless communication channels was proposed in [114]. The proposed model is able to capture the characteristics of time-varying HST wireless channels by using Markov chains to track the channel state variation at different received signal-to-noise ratio (SNR) intervals. However, the model has not been verified by using real-field measurements and thus deserves more investigation. The authors in [116] followed a similar approach to model the dynamic evolution of multi-path components, i.e., birth-death process, using a four-state Markov chain model. The four proposed states are no birth/death, births only, deaths only, and both births and deaths. The transition matrix of the birth-death process was calculated based on the measurement presented in [66]. Based on measurement of HST channels in viaduct and cutting scenarios, a finite-state Markov channel was also proposed in [123]. Simulation results showed that Ricean distribution can well characterize the measured amplitude of the small-scale fading in both HST scenarios and an NGSM can effectively capture the dynamic nature of the fast fading in HST channels.

IV. RESEARCH DIRECTIONS IN HST CHANNEL MEASUREMENTS AND MODELS

In this section, we will discuss important research directions that can be considered as guidelines for conducting future HST measurement campaigns and developing more realistic HST channel models.

A. Nonstationarity of HST Channels

Measurements in the literature have demonstrated that HST channels are non-stationary since the stationary conditions, measured by stationary interval, retain to a very short period of time in comparison with other types of channels, e.g., V2I and V2V channels [88]. This is mainly caused by the very high speed of the trains and the encountered changes in surrounding areas. Although the non-stationarity of HST channels has been implicitly considered in GBDMs [102]–[104], [106], but these models are mainly site-specific and cannot be easily generalized to a variety of scenarios. The non-stationarity feature of HST channels has been considered in the NGSM proposed in [114] by implementing the birth-death process to simulate the appearance and disappearance of the scatterers, and in RS-GBSMs in [109]–[112] by providing the time-variant functions of several channel model parameters, i.e., angular parameters, Doppler frequency, Ricean K-factor, and the distance between the Tx and Rx. However, verifying the proposed models by real-field measurements was only performed in [112] and therefore more comprehensive investigations are required to validate the accuracy of those models. Future non-stationary channel models should consider more time-variant model parameters, such as cluster powers and delays, and investigate the effect of the drift of scatterers into different delay taps on the non-stationarity of HST channels and the resulting correlation between these taps.

B. Statistical Properties of HST Channels

Investigating the statistical properties of HST channels is essential for understanding and analyzing HST communication systems. In Table I, several channel statistics obtained from measurements were presented. However, most of proposed HST channel models in the literature have failed to provide the corresponding theoretical analysis. In [107], the ST CCF was derived based on the proposed stationary narrowband HST channel model. In [111], a novel theoretical framework that characterizes non-stationary mobile fading channels in terms of their system functions and correlation functions was proposed. Based on this theoretical framework, different time-variant statistical properties of the RS-GBSMs in [111], [112] were derived, i.e., time-variant space CCFs, time-variant ACFs, time-variant space-Doppler (SD) power spectrum densities (PSDs), local scattering functions (LSFs) [111], and LCRs [112]. It is highly desirable to investigate the statistical properties of other HST channel models and further develop the aforementioned theoretical framework to include more statistical properties.

C. HST Scenarios

HST scenarios were classified and thoroughly explained in Section II of this article. During its travel and due to its high velocity, HST runs across diverse scenarios so rapidly that a single model is incapable of capturing accurately the variations of HST channels. While most standard channel models did not consider any of the HST scenarios, IMT-A channel model, WINNER II channel model, and most of the non-standard HST channel models were proposed for open space scenarios only. Due to the unique feature of tunnels, the propagation characteristics of signals inside tunnels are different from those of other HST scenarios. Conventional channel modeling techniques suitable for other HST scenarios are not directly applicable to tunnel scenarios. Moreover, research on channel modeling inside tunnels is yet to solve main problems such as the accurate characterization of multimode waveguide propagation and the determination of breakpoint for different propagation mechanisms inside tunnels. In addition, the research on 3D channel models for tunnels is still in its very early stages and accurate generic channel models that can be applied to different types of tunnel channels are still missing in the literature. Therefore, channel characterization and modeling for tunnel scenarios are still a quite challenging topic and need to be further investigated. Moreover, it is essential that future HST channel models consider other scenarios such as station scenarios that also have their unique channel characteristics, and preferably take into account the impact of diverse scenarios on HST channel models.

D. 3D HST Channel Models

Apart from the GBDMs that use 3D ray-tracing tool to model HST channels [103]–[106], HST channel models were generally proposed assuming that propagation waves are traveling in two dimensions and therefore ignore the impact of the elevation angle on channel statistics. In reality, radio waves propagate in three dimensions and scatterers are disperse in elevation, i.e., vertical plane, as well as in azimuth, i.e., horizontal plane. Recently, the 3GPP has developed a 3D channel model in urban microcell and urban macrocell scenarios following the framework of WINNER II channel model [124]. The proposed 3D 3GPP channel model introduced the zenith AoD and zenith AoA that are modeled by inverse Laplacian functions [125]. The 3D extensions of SCM and the WINNERII/WINNER+ channel models were proposed in [126] and [127], respectively, and an extension of the IMT-A channel model to the elevation plane was proposed in [128], [129]. However, none of the aforementioned channel models considered any of the HST scenarios. Thus, 3D channel measurements and models are necessary, especially when the HST is close to the BS where considering elevation angles can demonstrate the impact of the waves reflected from ground on the received signal.

E. HST-to-HST Communications

HST-to-HST communication has been proposed to enable HSTs exchange controlling and traffic information such as road obstacles and accidents via wireless communication links. A HST-to-HST communication model based on multihop and cooperation was proposed in [130]. In the proposed model, a source train uses trains on other tracks as relays to transmit signals to the destination train on the same track. Based on proposed HST-to-HST channel model, the bit error rate (BER) performance was investigated in [130] using the suburban scenario of COST 207 channel model and the outage capacity was analyzed in [131] using Nakagami-*m* channel model. Despite its importance as a safety measure to avoid accidents, the development of HST-to-HST channel models is still in its preliminary phase and further investigations are required.

F. System Performance

Investigating the performance of HST communication systems is the basis for system design and network planning. In [33], the HST communication system performance was investigated using data throughput to evaluate a seamless dual-link handover scheme. Another handover scheme was proposed in [34] and the system performance was evaluated by tracking the changes of throughput and signal-to-noise-and-interference ratio (SINR) over the time. The changes of SINR over the HST velocity were investigated in [132] to evaluate a transmit beamforming algorithm proposed for canceling the inter-channel interference (ICI) in HST communication systems. The performance of HST communication system that implements beamforming technique was also evaluated in [133] using measured throughput, SINR, and received signal strength indicator level. The deployment of DAS in HST communication systems was evaluated in [26] by using spectrum efficiency as a system performance metric. In [134], BER was used to evaluate a proposed radio resource allocation scheme for orthogonal frequency-division multiple access (OFDMA) HST systems. The BER performance of a HST communication system was also investigated in [135] where beamforming and Alamouti combined downlink transmission schemes were proposed. Mobile broadband performance experienced from regional HSTs was investigated in [136] by monitoring the fluctuation of system throughput caused by the varying distance between the BS and HST, multi-path fading, and co-channel interference conditions. A temporal proportional fair power allocation scheme for HST wireless communication systems was proposed in [137]. The proposed scheme was designed to achieve a trade-off between power efficiency and fairness along the time. HST channel capacity was analyzed in [138] to study the impact of different antenna array configurations on MIMO HST communication systems. In [139], the BER performance of spatial modulation systems was studied using the proposed non-stationary HST MIMO channel model in [111] with different HST scenarios. It was shown that the correlation between sub-channels, inter-symbol-interference, Doppler shift, and channel estimation errors are the main factors that affect the BER performance of SM systems under the HST channel model. More comprehensive system performance analysis that evaluates other schemes and considers more system performance indicators, e.g., capacity and quality of service (QoS), is required in the future.

V. CONCLUDING REMARKS

This article has provided a survey of HST channels in terms of conducted measurements and channel models. We have classified HST channel measurements according to scenarios, carrier frequencies, bandwidths, measured channels, antenna configurations, train speeds, and channel statistics. We have also presented various HST large-scale fading channel models in the literature. Then, we have classified HST small-scale fading channel models based on their modeling approaches, scenarios, stationarity, FS, and cellular architecture. Finally, we have highlighted some research directions in HST channel measurements and modeling. The discussions here will hopefully shed lights on recent challenges that face HST channels and help in conducting future measurement campaigns and developing more realistic HST channel models.

REFERENCES

[1] C.-X. Wang *et al.*, "Cellular architecture and key technologies for 5G wireless communication networks," *IEEE Commun. Mag.*, vol. 52, no. 2, pp. 122–130, Feb. 2014.

[2] A. F. Molisch, F. Tufvesson, J. Karedal, and C. F. Mecklenbrauker, "A survey on vehicle-to-vehicle propagation channels," *IEEE Wireless Commun.*, vol. 16, no. 6, pp. 12–22, Dec. 2009.

[3] C.-X. Wang, X. Cheng, and D. I. Laurenson, "Vehicle-to-vehicle channel modeling and measurements: Recent advances and future challenges," *IEEE Commun. Mag.*, vol. 47, no. 11, pp. 96–103, Nov. 2009.

[4] X. Cheng, C.-X. Wang, D. I. Laurenson, S. Salous, and A. V. Vasilakos, "An adaptive geometry-based stochastic model for non-isotropic MIMO mobile-to-mobile channels," *IEEE Trans. Wireless Commun.*, vol. 8, no. 9, pp. 4824–4835, Sep. 2009.

[5] X. Cheng *et al.*, "Cooperative MIMO channel modeling and multi-link spatial correlation properties," *IEEE J. Sel. Areas Commun.*, vol. 30, no. 2, pp. 388–396, Feb. 2012.

[6] X. Cheng, Q. Yao, M. Wen, C.-X. Wang, L. Song, and B. Jiao, "Wideband channel modeling and ICI cancellation for vehicle-to-vehicle communication systems," *IEEE J. Sel. Areas Commun.*, vol. 31, no. 9, pp. 434–448, Sep. 2013.

[7] Y. Yuan, C.-X. Wang, X. Cheng, B. Ai, and D. I. Laurenson, "Novel 3D geometry-based stochastic models for non-isotropic MIMO vehicle-to-vehicle channels," *IEEE Trans. Wireless Commun.*, vol. 13, no. 1, pp. 298–309, Jan. 2014.

[8] X. Cheng, C.-X. Wang, B. Ai, and H. Aggoune, "Envelope level crossing rate and average fade duration of non-isotropic vehicle-to-vehicle Ricean fading channels," *IEEE Trans. Intell. Transp. Syst.*, vol. 15, no. 1, pp. 62–72, Feb. 2014.

[9] Y. Yuan, C.-X. Wang, Y. He, M. M. Alwakeel, and H. Aggoune, "3D wideband non-stationary geometry-based stochastic models for non-isotropic MIMO vehicle-to-vehicle channels," *IEEE Trans. Wireless Commun.*, vol. 14, no. 2, pp. 6883–6895, Dec. 2015.

[10] Y. Fu *et al.*, "BER performance of spatial modulation systems under 3D V2V MIMO channel models," *IEEE Trans. Veh. Technol.*, 2015, submitted for publication.

[11] F. Abrishamkar and J. Irvine, "Comparison of current solutions for the provision of voice services to passengers on high speed trains," in *Proc. IEEE Veh. Technol. Conf. (VTC'00-Fall)*, Boston, MA, USA, Sep. 2000, pp. 1498–1505.

[12] D. T. Fokum and V. S. Frost, "A survey on methods for broadband Internet access on trains," *IEEE Commun. Surveys Tuts.*, vol. 12, no. 2, pp. 171–185, Apr. 2010.

[13] B. Ai *et al.*, "Challenges toward wireless communications for high-speed railway," *IEEE Trans. Intell. Transp. Syst.*, vol. 15, no. 5, pp. 2143–2158, Oct. 2014.

[14] M. Goller, "Application of GSM in high speed trains: Measurements and simulations," in *Proc. IEE Colloq. Radiocommun. Transp.*, May 1995, pp. 1–7.

[15] C. Briso, C. Cortes, F. J. Arques, and J. I. Alonso, "Requirements of GSM technology for the control of high speed trains," in *Proc. IEEE 13th IEEE Int. Symp. Pers. Indoor Mobile Radio Commun. (PIMRC'02)*, Lisbon, Portugal, Sep. 2002, pp. 792–793.

[16] K. Kastell, S. Bug, A. Nazarov, and R. Jakoby, "Improvements in railway communication via GSM-R," in *Proc. IEEE Veh. Technol. Conf. (VTC'06-Spring)*, Melbourne, VIC, Australia, May 2006, pp. 3026–3030.

[17] J. Calle-Sánchez, M. Molina-García, J. I. Alonso, and A. Fernández-Durán, "Long term evolution in high speed railway environments: Feasibility and challenges," *Bell Labs Tech. J.*, vol. 18, no. 2, pp. 237–253, Sep. 2013.

[18] K. Guan, Z. Zhong, and B. Ai, "Assessment of LTE-R using high speed railway channel model," in *Proc. 3rd Int. Conf. Commun. Mobile Comput. (CMC'11)*, Qingdao, China, Apr. 2011, pp. 461–464.

[19] J. Rodriguez-Pineiro *et al.*, "LTE downlink performance in high speed trains," in *Proc. IEEE Veh. Technol. Conf. (VTC'15-Spring)*, Glasgow, Scotland, May 2015, pp. 1–5.

[20] S. Zhang, M. Wu, and X. Lin, "Results and analysis based on a novel LTE-R channel measurement at 2.6 GHz," in *Proc. 22nd Int. Conf. Telecommun. (ICT'15)*, Sydney, NSW, Australia, Apr. 2015, pp. 403–407.

[21] M. Cheng, X. Fang, and W. Luo, "Beamforming and positioning-assisted handover scheme for long-term evolution system in high-speed railway," *IET Commun.*, vol. 6, no. 15, pp. 2335–2340, Oct. 2012.

[22] M. Alasali and C. Beckman, "LTE MIMO performance measurements on trains," in *Proc. 7th Eur. Conf. Antennas Propag. (EuCAP'13)*, Gothenburgh, Sweden, Apr. 2013, pp. 2327–2330.

[23] F. J. Martin-Vega, I. M. Delgado-Luque, F. Blanquez-Casado, G. Gomez, M. C. Aguayo-Torres, and J. T. Entrambasaguas, "LTE performance over high speed railway channel," in *Proc. IEEE Veh. Technol. Conf. (VTC'13-Fall)*, Las Vegas, NV, USA, Sep. 2013, pp. 1–5.

[24] 3GPP, "3rd Generation partnership project; Technical specification group radio access network; Evolved universal terrestrial radio access (E-UTRA); Base Station (BS) radio transmission and reception (Release 11)," TS36.104, V11.3.1, Jan. 2013.

[25] K. Yamada, Y. Sakai, T. Suzuki, Y. Kawahara, T. Asami, and H. Aida, "A communication system with a fast handover under a high speed mobile environment," in *Proc. IEEE Veh. Technol. Conf. (VTC'10-Fall)*, Ottawa, ON, Canada, Sep. 2010, pp. 1–5.

[26] J. Wang, H. Zhu, and N. J. Gomes, "Distributed antenna systems for mobile communications in high speed trains," *IEEE J. Sel. Areas Commun.*, vol. 30, no. 4, pp. 675–683, May 2012.

[27] H.-A. Hou and H.-H. Wang, "Analysis of distributed antenna system over high-speed railway communication," in *Proc. IEEE 23rd Int. Symp. Pers. Indoor Mobile Radio Commun. (PIMRC'12)*, Sydney, NSW, Australia, Sep. 2012, pp. 1300–1305.

[28] C. Yang, L. Lu, C. Di, and X. Fang, "An on-vehicle dual-antenna handover scheme for high-speed railway distributed antenna system," in *Proc. IEEE 60th Int. Conf. Wireless Commun. Netw. Mobile Comput. (WiCOM'10)*, Chengdu, China, Sep. 2010, pp. 1–4.

[29] D. Lee *et al.*, "Coordinated multipoint transmission and reception in LTE-advanced: Deployment scenarios and operational challenges," *IEEE Commun. Mag.*, vol. 50, no. 2, pp. 148–155, Feb. 2012.

[30] C.-X. Wang, X. Hong, X. Ge, X. Cheng, G. Zhang, and J. S. Thompson, "Cooperative MIMO channel models: A survey," *IEEE Commun. Mag.*, vol. 48, no. 2, pp. 80–87, Feb. 2010.

[31] Y. Zhou, Z. Pan, J. Hu, J. Shi, and X. Mo, "Broadband wireless communications on high speed trains," in *Proc. IEEE 20th Annu. Wireless Opt. Commun. Conf. (WOCC'11)*, Newark, NJ, USA, Apr. 2011, pp. 1–6.

[32] L. Tian, Y. Zhou, J. Li, Y. Huang, J. Shi, and J. Zhou, "A novel handover scheme for seamless wireless connectivity in high-speed rail," in *Proc. IEEE 7th Int. Conf. Wireless Mobile Comput. Netw. Commun. (WiMob'11)*, Wuhan, China, Oct. 2011, pp. 230–236.

[33] L. Tian, J. Li, Y. Huang, J. Shi, and J. Zhou, "Seamless dual-link handover scheme in broadband wireless communication systems for high-speed rail," *IEEE J. Sel. Areas Commun.*, vol. 30, no. 4, pp. 708–718, May 2012.

[34] O. B. Karimi, L. J. Liu, and C. Wang, "Seamless wireless connectivity for multimedia services in high speed trains," *IEEE J. Sel. Areas Commun.*, vol. 30, no. 4, pp. 729–739, May 2012.

[35] F. Haider *et al.*, "Spectral efficiency analysis of mobile femtocell based cellular systems," in *Proc. IEEE 13th Int. Conf. Commun. Technol. (ICCT'11)*, Jinan, China, Sep. 2011, pp. 347–351.

[36] F. Haider, C.-X. Wang, B. Ai, H. Haas, and E. Hepsaydir, "Spectral-energy efficiency trade-off of cellular systems with mobile femtocell deployment," *IEEE Trans. Veh. Technol.*, 2015, submitted for publication.

[37] X. Qian, H. Wu, and J. Meng, "A dual-antenna and mobile relay station based handover in distributed antenna system for high-speed railway," in *Proc. IEEE 7th Int. Conf. Innov. Mobile Internet Serv. Ubiq. Comput. (IMIS'13)*, Taichung, Taiwan, Jul. 2013, pp. 585–590.

[38] W. Luo, R. Zhang, and X. Fang, "A CoMP soft handover scheme for LTE systems in high speed railway," *EURASIP J. Wireless Commun. Netw.*, vol. 2012, 9 p., 2012, doi: 10.1186/1687-1499-2012-196.

[39] B. Lannoo, D. Colle, M. Pickavet, and P. Demeester, "Radio-over-fiber-based solution to provide broadband Internet access to train passengers," *IEEE Commun. Mag.*, vol. 45, no. 2, pp. 56–62, Feb. 2007.

[40] J.-Y. Zhang, Z.-H. Tan, and X.-X. Yu, "Coverage efficiency of radio-over-fiber network for high-speed railways," in *Proc. IEEE 6th Int. Conf. Wireless Commun. Netw. Mobile Comput. (WiCOM'10)*, Chengdu, China, Sep. 2010, pp. 1–4.

[41] ITU-R M.2135-1, "Guidelines for evaluation of radio interface technologies for IMT-advanced," Geneva, Switzerland, Rep. ITU-R M.2135-1, Dec. 2009.

[42] P. Kyösti *et al.*, "WINNER II channel models," IST-4-027756, WINNER II D1.1.2, v1.2, Apr. 2008.

[43] B. Ai *et al.*, "Radio wave propagation scene partitioning for high-speed rails," *Int. J. Antennas Propag.*, vol. 2012, 7 p., 2012, doi: 10.1155/2012/815232.

[44] 3GPP, "Universal mobile telecommunications system (UMTS); Radio frequency (RF) system scenarios (Release 12)," TR 25.942, version 12.0.0, Oct. 2014.

[45] L. Liu *et al.*, "The COST 2100 MIMO channel model," *IEEE Wireless Commun.*, vol. 19, no. 6, pp. 92–99, Dec. 2012.

[46] "Requirements for the radio interface(s) for international mobile telecommunications-2000 (IMT-2000)," ITU, Geneva, Switzerland, Tech. Rep. ITU-R M.1034-1, 2000.

[47] R. He, Z. Zhong, B. Ai, and K. Guan, "Reducing the cost of high-speed railway communications: From the propagation channel view," *IEEE Trans. Intell. Transp. Syst.* vol. 16, no. 4, pp. 2050–2060, Aug. 2015.

[48] J. Rodríguez-Piñeiro, J. A. García-Naya, Á. Carro-Lagoa, and L. Castedo, "A testbed for evaluating LTE in high-speed trains," in *Proc. IEEE Euromicro Conf. Digit. Syst. Des. (DSD'13)*, Santander, Spain, Sep. 2013, pp. 175–182.

[49] N. Kita *et al.*, "Experimental study of propagation characteristics for wireless communications in high-speed train cars," in *Proc. 3rd Eur. Conf. Antennas Propag. (EuCAP'09)*, Berlin, Germany, Mar. 2009, pp. 897–901.

[50] W. Dong, G. Liu, L. Yu, H. Ding, and J. Zhang, "Channel properties of indoor part for high-speed train based on wideband channel measurement," in *Proc. CHINACOM*, Beijing, China, Aug. 2010, pp. 1–4.

[51] M. Zhao *et al.*, "Analysis and modeling for train-ground wireless wideband channel of LTE on high-speed railway," in *Proc. IEEE Veh. Technol. Conf. (VTC'13-Spring)*, Dresden, Germany, Jun. 2013, pp. 1–5.

[52] R. Parviainen, P. Kyosti, Y. Hsieh, P. Ting, and J. Chiou, "Results of high speed train channel measurements," in *Proc. COST (TD'08)*, Lille, France, Oct. 2008.

[53] K. Pekka, "WINNER II channel models—Part II radio channel measurement and analysis results," IST-4-027756, WINNER II D1.1.2, v1.0, Sep. 2007.

[54] R. He *et al.*, "Measurement based channel modeling with directional antennas for high-speed railways," in *Proc. IEEE Wireless Commun. Netw. Conf. (WCNC'13)*, Shanghai, China, Apr. 2013, pp. 2932–2936.

[55] H. Wei, Z. Zhong, K. Guan, and B. Ai, "Path loss models in viaduct and plain scenarios of the high-speed railway," in *Proc. CHINACOM*, Beijing, China, Aug. 2010, pp. 1–5.

[56] J. Lu, G. Zhu, and B. Ai, "Radio propagation measurements and modeling in railway viaduct area," in *Proc. IEEE 6th Int. Conf. Wireless Commun. Netw. Mobile Comput. (WiCOM'10)*, Chengdu, China, Sep. 2010, pp. 1–5.

[57] L. Gao, Z. Zhong, B. Ai, and L. Xiong, "Estimation of the Ricean factor in K the high speed railway scenarios," in *Proc. CHINACOM*, Beijing, China, Aug. 2010, pp. 1–5.

[58] R. He, Z. Zhong, B. Ai, and J. Ding, "Distance-dependent model of Ricean K-factors in high-speed rail viaduct channel," in *Proc. IEEE Veh. Technol. Conf. (VTC'12-Fall)*, Québec City, QC, Canada, Sep. 2012, pp. 1–5.

[59] R. He, Z. Zhong, and B. Ai, "Path loss measurements and analysis for high-speed railway viaduct scene," in *Proc. 6th Int. Wireless Commun. Mobile Comput. Conf. (IWCMC'10)*, Caen, France, Jul. 2010, pp. 266–270.

[60] R. He, Z. Zhong, B. Ai, L. Xiong, and H. Wei, "A novel path loss model for high-speed railway viaduct scenarios," in *Proc. IEEE 7th Int. Conf. Wireless Commun. Netw. Mobile Comput. (WiCOM'11)*, Wuhan, China, Sep. 2011, pp. 1–4.

[61] R. He, Z. Zhong, B. Ai, L. Xiong, and J. Ding, "The effect of reference distance on path loss prediction based on the measurements in high-speed railway viaduct scenarios," in *Proc. CHINACOM*, Harbin, China, Aug. 2011, pp. 1201–1205.

[62] R. He, Z. Zhong, B. Ai, and J. Ding, "An empirical path loss model and fading analysis for high-speed railway viaduct scenarios," *IEEE Antennas Wireless Propag. Lett.*, vol. 10, pp. 808–812, Aug. 2011.

[63] H. Wei, Z. Zhong, L. Xiong, B. Ai, and R. He, "Study on the shadow fading characteristic in viaduct scenario of the high-speed railway," in *Proc. CHINACOM*, Harbin, China, Aug. 2011, pp. 1216–1220.

[64] B. Zhang, Z. Zhong, B. Ai, D. Yao, and R. He, "Measurements and modeling of cross-correlation property of shadow fading in high-speed railways," in *Proc. IEEE Veh. Technol. Conf. (VTC'14-Fall)*, Vancouver, BC, Canada, Sep. 2014, pp. 1–5.

[65] L. Gao, Z. Zhong, B. Ai, L. Xiong, and H. Zhang, "Analysis and emulation of the small-scale fading characteristics in the high-speed rail scenarios," in *Proc. CHINACOM*, Harbin, China, Aug. 2011, pp. 1181–1185.

[66] L. Liu *et al.*, "Position-based modeling for wireless channel on high-speed railway under a viaduct at 2.35 GHz," *IEEE J. Sel. Areas Commun.*, vol. 30, no. 4, pp. 834–845, May 2012.

[67] Y. Guo, J. Zhang, C. Zhang, and L. Tian, "Correlation analysis of high-speed railway channel parameters based on channel measurement," in *Proc. Int. Workshop High Mobility Wireless Commun. (HMWC'13)*, Shanghai, China, Nov. 2013, pp. 1–5.

[68] R. He, Z. Zhong, B. Ai, and J. Ding, "Measurements and analysis of short-term fading behavior for high-speed rail viaduct scenario," in *Proc. IEEE Int. Conf. Commun. (ICC'12)*, Ottawa, ON, Canada, Jun. 2012, pp. 4563–4567.

[69] R. He, Z. Zhong, B. Ai, G. Wang, J. Ding, and A. F. Molisch, "Measurements and analysis of propagation channels in high-speed railway viaducts," *IEEE Trans. Wireless Commun.*, vol. 12, no. 2, pp. 794–805, Feb. 2013.

[70] Q. Wang, C. Xu, M. Zhao, and D. Yu "Results and analysis for a novel 2x2 channel measurement applied in LTE-R at 2.6 GHz," in *Proc. IEEE Wireless Commun. Netw. Conf. (WCNC'14)*, Istanbul, Turkey, Apr. 2014, pp. 177–181.

[71] R. Sun, C. Tao, L. Liu, Z. Tan, L. Zhang, and T. Zhou, "Nonisotropic scattering characteristic in an alternant tree-blocked viaduct scenario on high-speed railway at 2.35 GHz," *Int. J. Antennas Propag.*, vol. 2014, 9 p., 2014, doi: 10.1155/2014/642894.

[72] T. Zhou, C. Tao, L. Liu, and Z. Tan, "A semiempirical MIMO channel model in obstructed viaduct scenarios on high-speed railway," *Int. J. Antennas Propag.*, vol. 2014, 10 p., 2014, doi: 10.1155/2014/287159.

[73] J. Lu, G. Zhu, and C. Briso-Rodriguez, "Fading characteristics in the railway terrain cuttings," in *Proc. IEEE Veh. Technol. Conf. (VTC'11-Spring)*, Budapest, Hungary, May 2011, pp. 1–5.

[74] R. He, Z. Zhong, B. Ai, and J. Ding, "Propagation measurements and analysis for high-speed railway cutting scenario," *Electron. Lett.*, vol. 47, no. 21, pp. 1167–1168, Oct. 2011.

[75] R. He, Z. Zhong, B. Ai, J. Ding, and Y. Yang, "Propagation measurements and analysis of fading behavior for high speed rail cutting scenarios," in *Proc. IEEE GLOBALCOM*, Anaheim, CA, USA, Dec. 2012, pp. 5015–5020.

[76] R. He, Z. Zhong, B. Ai, J. Ding, Y. Yang, and A. F. Molisch, "Short-term fading behavior in high-speed railway cutting scenario: Measurements, analysis, and statistical models," *IEEE Trans. Antennas Propag.*, vol. 61, no. 4, pp. 2209–2222, Apr. 2013.

[77] R. Sun, C. Tao, L. Liu, and Z. Tan, "Channel measurement and characterization for HSR U-shape groove scenarios at 2.35 GHz," in *Proc. IEEE Veh. Technol. Conf. (VTC'13-Fall)*, Las Vegas, NV, USA, Sep. 2013, pp. 1–5.

[78] L. Tian, J. Zhang, and C. Pan, "Small scale fading characteristics of wideband radio channel in the U-shape cutting of high-speed railway," in *Proc. IEEE Veh. Technol. Conf. (VTC'13-Fall)*, Las Vegas, NV, USA, Sep. 2013, pp. 1–6.

[79] F. Luan, Y. Zhang, L. Xiao, C. Zhou, and S. Zhou, "Fading characteristics of wireless channel on high-speed railway in hilly terrain scenario," *Int. J. Antennas Propag.*, vol. 2013, 9 p., 2013, doi: 10.1155/2013/378407.

[80] Y. Zhang, Z. He, W. Zhang, L. Xiao, and S. Zhou, "Measurement-based delay and Doppler characterizations for high-speed railway hilly scenario," *Int. J. Antennas Propag.*, vol. 2014, 8 p., 2014, doi: 10.1155/2014/875345.

[81] P. Aikio, R. Gruber, and P. Vainikainen, "Wideband radio channel measurements for train tunnels," in *Proc. IEEE Veh. Technol. Conf. (VTC'98)*, Ottawa, ON, Canada, May 1998, pp. 460–464.

[82] C. Briso-Rodriguez, J. M. Cruz, and J. I. Alonso, "Measurements and modeling of distributed antenna systems in railway tunnels," *IEEE Trans. Veh. Technol.*, vol. 56, no. 5, pp. 2870–2879, Sep. 2007.

[83] K. Guan, Z. Zhong, B. Ai, and T. Kürner, "Propagation measurements and analysis for train stations of high-speed railway at 930 MHz," *IEEE Trans. Veh. Technol.*, vol. 63, no. 8, pp. 3349–3516, Oct. 2014.

[84] K. Guan, Z. Zhong, B. Ai, and T. Kurner, "Empirical models for extra propagation loss of train stations on high-speed railway," *IEEE Trans. Antennas Propag.*, vol. 62, no. 3, pp. 1395–1408, Mar. 2014.

[85] J. Lu, G. Zhu, and B. Ai, "Fading analysis for the high speed railway viaduct and terrain cutting scenarios," *Int. J. Antennas Propag.*, vol. 2012, 9 p., 2012.

[86] K. Guan, Z. Zhong, B. Ai, and T. Kürner, "Propagation measurements and modeling of crossing bridges on high-speed railway at 930 MHz," *IEEE Trans. Veh. Technol.*, vol. 63, no. 8, pp. 502–517, Feb. 2014.

[87] Y. Wen, Y. Ma, X. Zhang, X. Jin, and F. Wang, "Channel fading statistics in high-speed mobile environment," in *Proc. IEEE APS Topical Conf. Antennas Propag. Wireless Commun. (APWC'12)*, Cape Town, South Africa, Sep. 2012, pp. 1209–1212.

[88] B. Chen, Z. Zhong, and B. Ai, "Stationarity intervals of time-variant channel in high speed railway scenario," *J. China Commun.*, vol. 9, no. 8, pp. 64–70, Aug. 2012.

[89] R. He, D. Zhong, B. Ai, and C. Oestges, "Shadow fading correlation in high-speed railway environments," *IEEE Trans. Veh. Technol.*, vol. 64, no. 7, pp. 2762–2772, Jul. 2015.

[90] R. He, Z. Zhong, B. Ai, and B. Zhang, "Measurement-based auto-correlation model of shadow fading for the high-speed railways in urban, suburban, and rural environments," in *Proc. Antennas Propag. Soc. Int. Symp. (APSURSI'14)*, Memphis, TN, USA, Jul. 2014, pp. 949–950.

[91] J. Qiu, C. Tao, L. Liu, and Z. Tan, "Broadband channel measurement for the high-speed railway based on WCDMA," in *Proc. IEEE Veh. Technol. Conf. (VTC'12-Spring)*, Yokohama, Japan, May 2012, pp. 1–5.

[92] L. Liu, C. Tao, T. Zhou, Y. Zhao, X. Yin, and H. Chen, "A highly efficient channel sounding method based on cellular communications for high-speed railway scenarios," *EURASIP J. Wireless Commun. Netw.*, vol. 2012, 16 p., 2012, doi: 10.1186/1687-1499-2012-307.

[93] X. Yin, X. Cai, X. Cheng, J. Chen, and M. Tian, "Empirical geometry-based random-cluster model for high-speed-train channels in UMTS networks," *IEEE Trans. Intell. Transp. Syst.*, vol. 16, no. 5, pp. 2850–2861, Oct. 2015.

[94] M. Dohler and Y. Li, *Cooperative Communications: Hardware, Channel & PHY*. Hoboken, NJ, USA: Wiley, 2010.

[95] D. Wang, L. Song, X. Kong, and Z. Zhang, "Near-ground path loss measurements and modeling for wireless sensor networks at 2.4 GHz," *Int. J. Distrib. Sensor Net.*, vol. 2012, 10 p., 2012, doi: 10.1155/2012/969712.

[96] K. Guan, Z. D. Zhong, J. I. Alonso, and C. Briso-Rodriguez, "Measurement of distributed antenna system at 2.4 GHz in a realistic subway tunnel environment," *IEEE Trans. Veh. Technol.*, vol. 61, no. 2, pp. 834–837, Feb. 2012.

[97] K. Guan, Z. D. Zhong, and B. Ai, "Statistic modeling for propagation in tunnels based on distributed antenna systems," in *Proc. IEEE Antennas Propag. Soc. Int. Symp. (APSURSI'13)*, Orlando, FL, USA, Jul. 2013, pp. 1920–1921.

[98] W. Qian, X. Chunxiu, W. Muqing, Z. Min, and Y. Deshui, "Propagation characteristics of high speed railway radio channel based on broadband measurements at 2.6 GHz," in *Proc. IEEE Wireless Commun. Netw. Conf. (WCNC'14)*, Istanbul, Turkey, Apr. 2014, pp. 166–170.

[99] T. Zhou, C. Tao, L. Liu, and Z. Tan, "Ricean K-factor measurements and analysis for wideband radio channels in high-speed railway U-shape cutting scenarios," in *Proc. IEEE Veh. Technol. Conf. (VTC'14-Spring)*, Seoul, Korea, May 2014, pp. 1–5.

[100] L. Tian and J. Zhang, "Analysis on non-stationary characteristics of wideband radio channel in HSR U-shape cutting scenario," in *Proc. IEEE Int. Conf. Commun. China (ICCC'14)*, Shanghai, China, Oct. 2014, pp. 544–548.

[101] J. Yang, B. Ai, and Z. Zhong "Construction and capacity analysis of high-rank LoS MIMO channels in high speed railway scenarios," *Int. J. Antennas Propag.*, vol. 2012, pp. 1–4, 2012, doi: 10.1155/2012/423759.

[102] L. Tian, X. Yin, Q. Zuo, J. Zhou, Z. Zhong, and S. Lu, "Channel modeling based on random propagation graphs for high speed railway scenarios," in *Proc. IEEE 23rd Int. Symp. Pers. Indoor Mobile Radio Commun. (PIMRC'12)*, Sydney, NSW, Australia, Sep. 2012, pp. 1746–1750.

[103] S. Knörzer, M. A. Baldauf, T. Fugen, and W. Wiesbeck, "Channel analysis for an OFDM-MISO train communications system using different antennas," in *Proc. IEEE Veh. Technol. Conf. (VTC'07-Fall)*, Baltimore, MD, USA, Oct. 2007, pp. 809–813.

[104] K. Guan, Z. Zhong, B. Ai, and T. Kürner, "Deterministic propagation modeling for the realistic high-speed railway environment," in *Proc. IEEE Veh. Technol. Conf. (VTC'13-Spring)*, Dresden, Germany, Jun. 2013, pp. 1–5.

[105] D. J. Cichon, T. C. Becker, and W. Wiesbeck, "Determination of time-variant radio links in high-speed train tunnels by ray optical modeling," in *Proc. IEEE Antennas Propag. Soc. Int. Symp. (APS/URSI'95)*, Newport Beach, CA, USA, Jun. 1995, pp. 508–511.

[106] D. J. Cichon, T. Zwick, and W. Wiesbeck, "Ray optical modeling of wireless communications in high-speed railway tunnels," in *Proc. IEEE Veh. Technol. Conf. (VTC'96-Spring)*, Atlanta, GA, USA, May 1996, pp. 546–550.

[107] B. Chen and Z. Zhong, "Geometry-based stochastic modeling for MIMO channel in high-speed mobile scenario," *Int. J. Antennas Propag.*, vol. 2012, 6 p., 2012, doi: 10.1155/2012/184682.

[108] Q. Zheng, C. Xu, and M. Wu, "A novel MIMO channel model for high speed railway system," in *Proc. IEEE Int. Conf. Commun. Technol. (ICCT'12)*, Chengdu, China, Nov. 2012, pp. 31–35.

[109] A. Ghazal, C.-X. Wang, H. Haas, M. A. Beach, X. Lu, and D. Yuan, "A non-stationary MIMO channel model for high speed train communication systems," in *Proc. IEEE Veh. Technol. Conf. (VTC'12-Spring)*, Yokohama, Japan, May 2012, pp. 1–5.

[110] A. Ghazal et al., "A non-stationary geometry-based stochastic model for MIMO high-speed train channels," in *Proc. 12th Int. Conf. ITS Telecommun. (ITST'12)*, Taipei, Taiwan, Nov. 2012, pp. 7–11.

[111] A. Ghazal, C.-X. Wang, B. Ai, D. Yuan, and H. Haas, "A non-stationary wideband MIMO channel model for high-mobility intelligent transportation systems," *IEEE Trans. Intell. Transp. Syst.*, vol. 16, no. 2, pp. 885–897, Apr. 2015.

[112] A. Ghazal, C.-X. Wang, Y. Liu, P. Fan, and M. K. Chahine, "A generic non-stationary MIMO channel model for different high-speed train scenarios," in *Proc. IEEE Int. Conf. Commun. China (ICCC'15)*, Shenzhen, China, Nov. 2015.

[113] B. Chen, Z. Zhong, B. Ai, and D. Michelson, "A geometry-based stochastic channel model for high-speed railway cutting scenarios," *IEEE Antennas Wireless Propag. Lett.*, vol. 14, pp. 851–854, Apr. 2015.

[114] S. Lin, Z. Zhong, L. Cai, and Y. Luo, "Finite state Markov modelling for high speed railway wireless communication channel," in *Proc. IEEE GLOBECOM*, Anaheim, CA, USA, Dec. 2012, pp. 5421–5426.

[115] S. Lin et al., "Finite-state Markov modeling for high-speed railway fading channels," *IEEE Antennas Wireless Propag. Lett.*, vol. 14, pp. 954–957, Apr. 2015.

[116] L. Liu, C. Tao, J. Qiu, T. Zhou, R. Sun, and H. Chen, "The dynamic evolution of multipath components in high-speed railway in viaduct scenarios: From the birth-death process point of view," in *Proc. IEEE 23rd Int. Symp. Pers. Indoor Mobile Radio Commun. (PIMRC'12)*, Sydney, NSW, Australia, Sep. 2012, pp. 1774–1778.

[117] Y. Liu, C.-X. Wang, A. Ghazal, S. Wu, and W. Zhang, "A multi-mode waveguide tunnel channel model for high-speed train wireless communication systems," in *Proc. 9th Eur. Conf. Antennas Propag. (EuCAP'15)*, Lisbon, Portugal, Apr. 2015, pp. 1–5.

[118] R. He, Z. Zhong, and C. Briso, "Broadband channel long delay cluster measurements and analysis at 2.4 GHz in subway tunnels," in *Proc. IEEE Veh. Technol. Conf. (VTC'11-Spring)*, Budapest, Hungary, May 2011, pp. 1–5.

[119] K. Guan, Z. Zhong, B. Ai, and T. Kurner, "Semi-deterministic path-loss modeling for viaduct and cutting scenarios of high-speed railway," *IEEE Antennas Wireless Propag. Lett.*, vol. 12, pp. 789–792, Jun. 2013.

[120] C.-X. Wang, M. Ptzold, and Q. Yao, "Stochastic modeling and simulation of frequency correlated wideband fading channels," *IEEE Trans. Veh. Technol.*, vol. 56, no. 3, pp. 1050–1063, May 2007.

[121] M. Patzold, *Mobile Radio Channels*, 2nd ed. Hoboken, NJ, USA: Wiley, 2011.

[122] R. He, B. Ai, Z. Zhong, A. F. Molisch, R. Chen, and Y. Yang, "A measurement-based stochastic model for high-speed railway channels," *IEEE Trans. Intell. Transp. Syst.*, vol. 16, no. 3, pp. 1120–1135, Jun. 2015.

[123] L. Xuan, S. Chao, B. Ai, and Z. Gang, "Finite-state Markov modeling of fading channels: A field measurement in high-speed railways," in *Proc. IEEE Int. Conf. Commun. China (ICCC'13)*, Xi'an, China, Aug. 2013, pp. 577–582.

[124] 3GPP TR 36.873 V12.2.0, "Study on 3D channel model for LTE," Jun. 2015.

[125] B. Mondal et al., "3D channel model in 3GPP," *IEEE Commun. Mag.*, vol. 53, no. 3, pp. 16–23, Mar. 2015.

[126] M. Shafi, M. Zhang, P. J. Smith, A. L. Moustakas, and A. F. Molisch, "The impact of elevation angle on MIMO capacity," in *Proc. IEEE Int. Conf. Coomun. (ICC'06)*, Istanbul, Turkey, Jun. 2006, pp. 4155–4160.

[127] J. Meinila *et al.*, "D5.3: WINNER+ final channel models," CELTIC/CP5-026, Jun. 2010.

[128] T. A. Thomas, F. W. Vook, E. Mellios, G. S. Hilton, A. R. Nix, and E. Visotsky, "3D extension of the 3GPP/ITU channel model," in *Proc. IEEE Veh. Technol. Conf. (VTC'13-Spring)*, Dresden, Germany, Jun. 2013, pp. 1–5.

[129] R. Almesaeed, A. S. Ameen, E. Mellios, A. Doufexi, and A. R. Nix, "A proposed 3D extension to the 3GPP/ITU channel model for 800 MHz and 2.6 GHz bands," in *Proc. 8th Eur. Conf. Antennas Propag. (EuCAP'14)*, The Hague, The Netherlands, Apr. 2014, pp. 3039–3043.

[130] P. Liu, B. Ai, Z. Zhong, and X. Zhou, "A novel train-to-train communication model design based on multihop in high-speed railway," *Int. J. Antennas Propag.*, vol. 2012, 9 p., 2012, doi: 10.1155/2012/475492.

[131] P. Liu, X. Zhou, and Z. Zhong, "Outage analysis of train-to-train communication model over Nakagami-m channel in high-speed railway," *Int. J. Antennas Propag.*, vol. 2013, 10 p., 2013, doi: 10.1155/2013/617895.

[132] Q. Luo, W. Fang, T. Yang, and D. Wang, "A transmit beamforming algorithm for high-speed train communication," in *Proc. IEEE Veh. Technol. Conf. (VTC'12-Fall)*, Québec City, QC, Canada, Sep. 2012, pp. 1–5.

[133] H.-H. Wang and H.-A. Hou, "Experimental analysis of beamforming in high-speed railway communication," in *Proc. IEEE 22nd Int. Symp. Pers. Indoor Mobile Radio Commun. (PIMRC'11)*, Toronto, ON, Canada, Sep. 2011, pp. 745–749.

[134] H. Zhu, "Radio resource allocation for OFDMA systems in high speed environments," *IEEE J. Sel. Areas Commun.*, vol. 30, no. 4, pp. 748–759, May 2012.

[135] M. Cheng, X. Fang, and L. Yan, "Beamforming and Alamouti STBC combined downlink transmission schemes in communication systems for high-speed railway," in *Proc. Int. Conf. Wireless Commun. Signal Process. (WCSP'13)*, Hangzhou, China, Oct. 2013, pp. 1–6.

[136] J. Yao, S. S. Kanhere, and M. Hassan, "Mobile broadband performance measured from high-speed regional trains," in *Proc. IEEE Veh. Technol. Conf. (VTC'11-Fall)*, San Francisco, CA, USA, Sep. 2011, pp. 1–5.

[137] Y. Dong, P. Fan, and K. Letaief, "High speed railway wireless communications: Efficiency v.s. fairness," *IEEE Trans. Veh. Technol.*, vol. 63, no. 2, pp. 925–930, Feb. 2014.

[138] B. Chen, Z. Zhong, B. Ai, and X. Chen, "Comparison of antenna arrays for MIMO system in high speed mobile scenarios," in *Proc. IEEE Veh. Technol. Conf. (VTC'11-Spring)*, Budapest, Hungary, May 2011, pp. 1–5.

[139] Y. Fu, C.-X. Wang, A. Ghazal, H. Aggoune, and M. M. Alwakeel, "Performance investigation of spatial modulation systems under nonstationary wideband high-speed train channel models," *IEEE Trans. Wireless Commun.*, submitted for publication.

Cheng-Xiang Wang (S'01–M'05–SM'08) received the B.Sc. and M.Eng. degrees in communication and information systems from Shandong University, Jinan, China, and the Ph.D. degree in wireless communications from Aalborg University, Aalborg, Denmark, in 1997, 2000, and 2004, respectively. He has been with Heriot-Watt University, Edinburgh, U.K., since 2005, and was promoted to a Professor of wireless communications in 2011. He is also an Honorary Fellow with the University of Edinburgh, Edinburgh, U.K., and a Chair/Guest Professor with Shandong University and Southeast University, Nanjing, China. He was a Research Fellow with the University of Agder, Grimstad, Norway, from 2001 to 2005, a Visiting Researcher at Siemens AG-Mobile Phones, Munich, Germany, in 2004, and a Research Assistant with the Technical University of Hamburg-Harburg, Hamburg, Germany, from 2000 to 2001. He has edited one book and published over 230 papers in refereed journals and conference proceedings. His research interests include wireless channel modelling and 5G wireless communication networks, including green communications, cognitive radio networks, high mobility communication networks, massive MIMO, millimeter wave communications, and visible light communications. He served or is currently serving as an Editor for international journals, including the IEEE TRANSACTIONS ON VEHICULAR TECHNOLOGY (since 2011), the IEEE TRANSACTIONS ON COMMUNICATIONS (since 2015), and the IEEE TRANSACTIONS ON WIRELESS COMMUNICATIONS (2007–2009). He was the leading Guest Editor for the IEEE JOURNAL ON SELECTED AREAS IN COMMUNICATIONS (special issue on Vehicular Communications and Networks). He is a Fellow of the IET and the HEA, and a member of EPSRC Peer Review College. He served or is serving as a TPC member, the TPC Chair, and the General Chair for over 80 international conferences. He was the recipient of Best Paper Awards from the IEEE GLOBECOM 2010, the IEEE ICCT 2011, the ITST 2012, the IEEE VTC 2013-Spring, and the IWCMC 2015.

Ammar Ghazal (S'15) received the B.Sc. degree in electronics and telecommunication engineering from Damascus University, Damascus, Syria, and the M.Sc. and Ph.D. degrees from Heriot-Watt University, Edinburgh, U.K., in 2006, 2010, and 2015, respectively. His research interests include wireless propagation channel characterization and modeling, nonstationary channel models, and high-speed train wireless propagation.

Bo Ai (M'00–SM'09) received the master's and Ph.D. degrees from Xidian University, Xi'an, China, in 2002 and 2004, respectively. He is currently working with Beijing Jiaotong University, Beijing, China, as a Professor and an Advisor of Ph.D. candidates. He is the Deputy Director of State Key Laboratory of Rail Traffic Control and Safety, Beijing Jiaotong University. He has authored/coauthored five books, 26 invention patents, and 220 scientific research papers in his research area till now. His research interests include broadband and dedicated mobile communication theories and technologies for GSM-R and LTE-R, with emphasis on channel measurements and modeling. He received the Excellent Postdoctoral Research Fellow (with great Hons.) from Tsinghua University, Beijing, China, in 2007. He is a Fellow of the IET. He is an Associate Editor for the IEEE TRANSACTIONS ON CONSUMER ELECTRONICS and an Editorial Committee Member of the journal, *Wireless Personal Communications*.

Yu Liu received the B.Sc. and M.Eng. degrees in communication and information systems from Qufu Normal University, Qufu, China, in 2010 and 2013, respectively. She is currently pursuing the Ph.D. degree at the School of Information Science and Engineering (ISE), Shandong University, Jinan, China. Her research interests include nonstationary channel modeling, high-speed train wireless propagation characterization and modeling, and channel modeling for special scenarios.

Pingzhi Fan (M'93–SM'99–F'15) received the Ph.D. degree in electronic engineering from Hull University, Kingston upon Hull, U.K. He is currently a Professor and the Director of the Institute of Mobile Communications, Southwest Jiaotong University, Chengdu, China. He was the Chief Scientist of a National 973 Research Project. He has over 200 research papers published in various academic English journals (IEEE/IEE/IEICE, etc.), and eight books (including edited), and is the inventor of 20 granted patents. His research interests include high mobility wireless communications, 5G technologies, wireless networks for big data, and signal design and coding. He served as the General Chair or TPC chair of a number of international conferences, and has been the Guest Editor-in-Chief, the Guest Editor or the Editorial Member of several international journals. He is the Founding Chair of the IEEE VTS BJ Chapter and ComSoc CD Chapter, the Founding Chair of the IEEE Chengdu Section. He also served as a Board Member of the IEEE Region 10, the IET (IEE) Council and the IET Asia-Pacific Region. He was a recipient of the U.K. ORS Award and the Outstanding Young Scientist Award by NSFC.